Immobilization of the Type XIV Myosin Complex in *Toxoplasma gondii*Ⓓ

Terezina M. Johnson, Zenon Rajfur, Ken Jacobson, and Con J. Beckers

Department of Cell and Developmental Biology, The University of North Carolina, Chapel Hill, NC 27599-7090

The substrate-dependent movement of apicomplexan parasites such as *Toxoplasma gondii* and *Plasmodium* sp. is driven by the interaction of a type XIV myosin with F-actin. A complex containing the myosin-A heavy chain, a myosin light chain, and the accessory protein GAP45 is attached to the membranes of the inner membrane complex (IMC) through its tight interaction with the integral membrane glycoprotein GAP50. For the interaction of this complex with F-actin to result in net parasite movement, it is necessary that the myosin be immobilized with respect to the parasite and the actin with respect to the substrate the parasite is moving on. We report here that the myosin motor complex of *Toxoplasma* is firmly immobilized in the plane of the IMC. This does not seem to be accomplished by direct interactions with cytoskeletal elements. Immobilization of the motor complex, however, does seem to require cholesterol. Both the motor complex and the cholesterol are found in detergent-resistant membrane domains that encompass a large fraction of the inner membrane complex surface. The observation that the myosin XIV motor complex of *Toxoplasma* is immobilized within this cholesterol-rich membrane likely extends to closely related pathogens such as *Plasmodium* and possibly to other eukaryotes.

INTRODUCTION

Members of the phylum Apicomplexa are pathogenic protozoan parasites of humans and animals. They include *Plasmodium falciparum*, the causative agent of malaria, and *Toxoplasma gondii*, which causes severe disease in immunocompromised humans and congenital disease in infants (Dubey, 1994). The life cycle of apicomplexan parasites alternates between a motile extracellular phase during which they do not replicate and a nonmotile phase within host cells where growth and replication occur. The ability of these parasites to invade host cells is therefore critical for their survival. Their ability to egress from dying host cells after multiple rounds of replication is equally important, however, because this ensures survival and spread of the parasites. Both invasion and egress are dependent on active motility of the parasite (Meissner *et al.*, 2002). The type of motility seen in apicomplexan parasites is very unusual, because it does not require typical locomotive organelles, such as filipodia or flagellae, but instead it involves a unique substrate-dependent type of movement called gliding motility.

Gliding motility is dependent on the interaction of actin filaments and the type XIV myosin TgMyoA located in the parasite pellicle between the plasma membrane and inner membrane complex (IMC) (Heintzelman and Schwartzman,

Ⓓ The online version of this article contains supplemental material at *MBC Online* (http://www.molbiolcell.org).

Address correspondence to: Con J. Beckers (cbeckers@med.unc.edu).

Abbreviations used: CE, cholesteryl; DRM, detergent-resistant membrane; FRAP, fluorescence recovery after photobleaching; IMC, inner membrane complex; mβCD, methyl-β-cyclodextrin; PC, phosphocholine; TLC, thin layer chromatography.

1999; Meissner *et al.*, 2002; Supplemental Figure 1). Depolymerization of the actin filaments with cytochalasin D or inhibition of myosin ATPase activity with butanedione monoxime blocks motility and host cell invasion completely, indicating the importance of actin–myosin interactions for the survival of the parasite (Dobrowolski and Sibley, 1996; Meissner *et al.*, 2002). Direct evidence for the essential role of TgMyoA in *Toxoplasma* motility and survival has come from elegant experiments in which expression of the MyoA gene was down-regulated, resulting in prominent defects in parasite motility and survival (Meissner *et al.*, 2002).

For the interaction of actin with myosin to result in net movement of a parasite with respect to its substrate, it is essential that myosin is immobilized with respect to the parasite and the actin with respect to the substrate. For the F-actin in *Toxoplasma* and *Plasmodium*, this seems to be accomplished through its interaction with the glycolytic enzyme aldolase, which, in turn, interacts with MIC2/TRAP (Supplemental Figure 1). Because the latter are cell surface adhesins that can mediate parasite attachment to host cells or extracellular matrix components, the actin-MIC2/TRAP–substrate interactions seem to be sufficient for immobilization of parasite F-actin filaments. (Jewett and Sibley, 2003; reviewed in Soldati and Meissner, 2004).

TgMyoA, in contrast, has recently been shown to be associated with the IMC in a hetero-oligomeric complex called the glideosome (Gaskins *et al.*, 2004). In addition to TgMyoA, this complex consists of a myosin light chain (TgMLC1) (Herm-Gotz *et al.*, 2002) and two novel proteins, TgGAP45 and TgGAP50 (Gaskins *et al.*, 2004). A similar complex has also been described in *Plasmodium* (Bosch *et al.*, 2006), and it is also found associated with the IMC (Bergman *et al.*, 2003; Bosch *et al.*, 2006). Whereas TgGAP45 seems to be an essential protein, its exact function in glideosome activity or membrane anchoring is not clear. TgGAP50, in contrast, is an integral membrane glycoprotein of the IMC membranes,

and it is essential for anchoring of the glideosome in those membranes (Gaskins *et al.*, 2004). These proteins that make up the glideosome are conserved across the apicomplexan phylum, indicating a common molecular mechanism for motility (Kappe *et al.*, 1999; Baum *et al.*, 2006).

For net parasite movement to occur, it is not sufficient, however, for the glideosome to be merely associated with a membrane. It is also critical that the glideosome is immobilized within the plane of the IMC membrane. Here, we show that the glideosome is indeed immobilized within the plane of the IMC. We have found no evidence for the involvement of other IMC-associated proteins in this immobilization. Instead, it seems that the lipid environment in the IMC, and specifically the presence of cholesterol, is an important factor in glideosome immobilization.

MATERIALS AND METHODS

Culture of Toxoplasma

The RH (HXGPRT−) strain of *T. gondii* and its derivatives expressing various fusion proteins were maintained in human foreskin fibroblasts (HFFs) as described previously (Gaskins *et al.*, 2004). Metabolic labeling of parasite proteins was performed as described previously (Gaskins *et al.*, 2004). Parasites were isolated from recently lysed cultures by passage through 18- and 25-gauge needles and centrifugation at room temperature for 5 min at $800 \times g$. Parasites were resuspended in phosphate-buffered saline (PBS) and passed through 5-μm filters to remove the small amount of host cell debris, and they were collected again by centrifugation as described above.

Reagents

The generation of monospecific antisera to *Toxoplasma* IMC1 has been described previously (Mann *et al.*, 2002). Monospecific antisera to yellow fluorescent protein (YFP) were generated by injecting rabbits with purified recombinant YFP (Cocalico Biologicals, Reamstown, PA). 2-(4,4-Difluoro-5,7-diphenyl-4-bora-3*a*,4*a*-diaza-*s*-indacene-3-pentanoyl)-1-hexadecanoyl-*sn*-glycero-3-phosphocholine (BODIPY-PC) and cholesteryl 4,4-difluoro-5,7-dimethyl-4-bora-3*a*,4*a*-diaza-*s*-indacene-3-dodecanoate (BODIPY-cholesteryl) were obtained from Invitrogen (Carlsbad, CA). Methyl-β-cyclodextrin (mβCD) was purchased from Sigma-Aldrich (St. Louis, MO).

Fluorescence Recovery after Photobleaching (FRAP) Experiments

FRAP measurements were performed on a custom-built system based on a Leitz microscope (Leica Microsystems, Bannockburn, IL) and Spectra Physics 164 argon ion laser (488-nm line; Spectra Physics, Mountain View, CA). The laser beam was focused to a 3.4-μm spot ($1/e^2$) by using a $40\times$ oil immersion objective (1.3 numerical aperture [NA]). The power of the bleaching beam was optimized for specimen spot photobleaching and varied from 50 to 300 mW (measured at the laser output). Fluorescence signals were detected by EMI cooled photomultiplier (S 20 photocathode; EMI, Hayes, United Kingdom) working in single photon counting mode. FRAP curves were obtained by collecting PMT signal in a multichannel scaler card (Ortec, Oak Ridge TN). Diffusion coefficients and immobile fraction were obtained by numerical analysis of FRAP curves by using custom-written software (Gordon *et al.*, 1998). Cells on coverslips were mounted in custom-made airtight chambers. Video-FRAP was performed on an Olympus microscope (Olympus, Center Valley, PA). The laser beam from a Spectra Physics Stabilite 2017 argon ion laser was focused to an ~3-μm spot by using $100\times$ oil immersion objective (1.25 NA). Images were collected by Hamamatsu 4880 cooled charge-couple device (CCD) camera (Hamamatsu, Bridgewater, NJ) driven by MetaMorph imaging software (Molecular Devices, Sunnyvale, CA). Cells were kept in a 37°C environmental chamber (Warner Instruments, Hamden, CT), and CO_2 was flushed over the culture dishes.

Differential Detergent Extraction of Toxoplasma Membranes

Purified parasites (3×10^7) were extracted for 10 min on ice in Triton X (TX)100/PBS (1% Triton X-100, 154 mM NaCl, 1.54 mM KH_2PO_4, and 2.71 mM Na_2HPO_4, pH 7.4) in the presence of protease inhibitors (Sigma-Aldrich). The TX100/PBS-soluble and -insoluble material was collected by centrifugation at $14,000 \times g$ for 15 min at 4°C. The TX100/PBS-insoluble material was subsequently extracted for 10 min on ice in TX100/TBS (1% Triton X-100, 150 mM NaCl, and 25 mM Tris-HCl, pH 7.4) in the presence of protease inhibitors, and the TX100/TBS-soluble and-insoluble material was collected by centrifugation as described above.

Transmission Electron Microscopy

Parasites were treated as described above in either TX100/PBS, TX100/TBS, or TX100/PBS plus mβCD. Insoluble parasite material was incubated in 1% glutaraldehyde (Electron Microscopy Sciences, Hatfield, PA) in PBS for 20 min on ice. Parasites were washed in PBS and collected by centrifugation at $16,000 \times g$ for 10 min at 4°C. Parasites were then resuspended in 1% tannic acid (Electron Microscopy Sciences) for 20 min on ice, washed again, and incubated in 1% OsO_4 (Electron Microscopy Sciences) for 20 min at room temperature. Parasites were washed twice in PBS, dehydrated in a 50–100% ethanol series, and after two washes propylene oxide embedded in Epon. The polymerized blocks were sectioned at 60 nm with a Leica Ultracut UCT ultramicrotome (Leica Microsystems). Sections were stained with 2% uranyl acetate and Sato's lead stain, and they were viewed on an FEI Tecnai 12 electron microscope (FEI, Hillsboro, OR). Images were collected with a Gatan model 794 multiscan digital camera (Gatan, Pleasanton, CA).

Fluorescent Lipid Labeling

Parasites were incubated in either 10 μM BODIPY-PC or BODIPY-cholesteryl for 3 h at 37°C in intracellular buffer (Moudy *et al.*, 2001). Cells were washed once in PBS and collected by centrifugation for 5 min at $800 \times g$. Parasites were extracted in TX100/PBS or TX100/TBS at 4°C for 10 min in the presence of 5 μM BODIPY-CE or BODIPY-PC for lipid labeling.

Thin Layer Chromatography

Parasites ($6–9 \times 10^8$) were isolated and extracted as described above to obtain subcellular fractions. Lipids were extracted in chloroform/methanol by the method of Bligh and Dyer (1959) and separated by monodimensional thin layer chromatography (TLC) on Partisil LK6D silica gel 60 A plates (Whatman, Clifton, NJ). Lipids were separated in a solvent system composed of hexane:ether:acetic acid (70:30:1) for cholesterol and methanol:chloroform: ammonium hydroxide:water (60:72:7.5:10.5) for phospholipids. Authentic cholesterol standard (Avanti Polar Lipids, Alabaster, AL) was run in parallel, and all cholesterol was visualized by spraying with 3% cupric acetate in 8% H_3PO_4 and baking at 100°C for 1 h. Fluorescent lipids were detected by exposure to 450- and 635-nm light with a STORM Scanner Control Version 5.03 (GE Healthcare, Little Chalfont, Buckinghamshire, United Kingdom) and visualized with ImageQuant TL software (GE Healthcare).

Cholesterol Depletion of the Toxoplasma IMC Membranes

Parasites were extracted in TX100/PBS for 10 min at 4°C in the presence of protease inhibitors, and the TX100/PBS-resistant fraction was collected by centrifugation at $9400 \times g$ for 10 min at 4°C. This material was subsequently resuspended in either PBS, 30 mM mβCD in PBS, or 30 mM mβCD with 5 μg of cholesterol in PBS and incubated at 37°C for 45 min. Extraction of the glideosome under these conditions was monitored by fluorescence microscopy and differential centrifugation. For fluorescence microscopy, an aliquot of the treated and untreated parasites were washed once in PBS, and then it was allowed to adhere to poly-L-lysine–coated coverslips. TX100 was added to the remainder of the reactions to a final concentration of 1%, and, after a-10 min incubation at 4°C, the soluble and insoluble material was separated by centrifugation for 10 min at $9400 \times g$ at 4°C and analyzed by SDS-polyacrylamide gel electrophoresis (PAGE) and immunoblot.

Sucrose Gradient Centrifugation

Parasites ($2–4 \times 10^8$) were lysed in TX100/PBS for 10 min on ice in the presence of protease inhibitors. Material was divided into two aliquots, and it was centrifuged at $9400 \times g$ for 10 min at 4°C. The TX/PBS-resistant material was incubated in PBS in the presence or absence of mβCD as described above, followed by the addition of TX100 to a final concentration of 1% and an additional incubation on ice for 20 min. Samples were then adjusted to a total volume of 500 μl and 1.6 M sucrose, transferred to 13- $\times$ 51-mm centrifuge tubes (Beckman Coulter, Fullerton, CA), and overlaid with 500 μl each of 1.4, 1.2, 1.1, 1.0, 0.9, 0.8, 0.7, and 0.6 M, and 1 ml of 0.25 M sucrose. Gradients were centrifuged for 2 h at $120,000 \times g$ and 4°C in a MLS-50 swinging bucket rotor (Beckman Coulter, Fullerton, CA). Fractions (500 μl) were collected from the bottom, and pellets were resuspended in 500 μl of PBS for analysis by Western blot.

Fluorescence Microscopy

Cells labeled with fluorescent lipids were allowed to adhere to poly-L-lysine–coated coverslips, and they were fixed with 3% paraformaldehyde in PBS for 7 min at room temperature. For immunofluorescence, cells were permeabilized in 0.5% TX100 in PBS for 7 min at room temperature, and then they were incubated with primary antibody (rabbit α-IMC1) for 30 min in 3% bovine serum albumin (BSA) in PBS. Samples were washed and incubated with Alexa Fluor 350-conjugated secondary antibodies (Invitrogen) in 3% BSA in PBS for 30 min at room temperature. Images were captured using an epifluorescence Nikon Eclipse TE-2000 microscope (Nikon, Melville, NY) and a Hamamatsu 1394 cooled digital CCD camera (Hamamatsu) and Metamorph
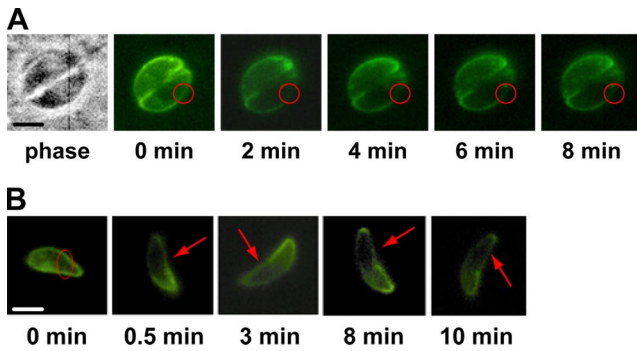
Figure 1. GAP50 is immobilized within the inner membrane complex of *T. gondii*. (A) Parasites stably expressing GAP50-YFP were allowed to infect HFF cells. In these video-FRAP experiments, pre-bleach images were captured and fluorescence at the indicated portion of the IMC was photobleached. Images were taken at 2-min intervals thereafter to monitor diffusion into the bleached region. (B) FRAP on motile extracellular parasites also demonstrated that GAP50-YFP is immobilized. Parasites were harvested and allowed to move along poly-L-lysine–coated coverslips during FRAP analysis. Bars, 5 μm.

imaging software (Molecular Devices). Adobe Photoshop (Adobe Systems, San Jose, CA) was used to crop images.

SDS-PAGE and Immunoblotting

Protein preparations were separated by SDS-PAGE on 10% polyacrylamide mini gels. Transfer to nitrocellulose and immunoblot analysis was performed as described previously (Mann and Beckers, 2001).

RESULTS

TgGAP50 Is Immobilized in the Inner Membrane Complex of Toxoplasma

TgGAP50 is an integral membrane glycoprotein that anchors the glideosome to the IMC membrane (Gaskins *et al.*, 2004).

For net movement to be achieved by the parasite, the prediction would be that TgGAP50 is immobilized within the plane of this membrane. To test this hypothesis, we used FRAP to determine the extent to which a functional but fluorescent derivative of TgGAP50, TgGAP50-YFP, is able to move within the plane of the IMC membrane. Intracellular parasites stably expressing TgGAP50-YFP were bleached in small regions at different locations of the IMC membrane. Images taken at 30-s time intervals for up to 8 min thereafter reveal that TgGAP50-YFP does not migrate into bleached regions, indicating that the protein is indeed immobilized in intracellular *Toxoplasma* (Figure 1A). To determine whether TgGAP50 motility is increased when parasites are actually moving, we repeated the same experiments on motile, extracellular *Toxoplasma*. As can be seen in Figure 1B, no diffusion of TgGAP50-YFP was observed in actively moving parasites, indicating that the protein is immobilized within the plane of the IMC in both intracellular and extracellular parasites. As a control, we used a TgGAP45–YFP fusion protein, which, unlike TgGAP50–YFP, does not associate with the other members of the glideosome (Supplemental Figure 2). Like wild-type GAP45, however, GAP45-YFP is also associated with the membrane of the IMC due to N-terminal palmitoylation and myristoylation of the protein (Johnson, DeVore, and Beckers, unpublished data). A similar modification has also been described for the protein found in *Plasmodium* (Rees-Channer *et al.*, 2006). FRAP analysis on TgGAP45–YFP demonstrates that the protein is able to diffuse freely along the IMC (Figure 2A). As an additional control, cytoplasmic green fluorescent protein (GFP) was transiently expressed in COS7 cells in which fluorescence also recovered after photobleaching (Figure 2A). Further quantitative analysis indicates the recovery time of the TgGAP50-YFP mobile fraction was much slower than those of the controls, showing a diffusion coefficient of 0.019 μm^2/s (Figure 2B). On average, TgGAP50-YFP had a mobile fraction of only 16.1% compared with 60.3 and 92.8% for
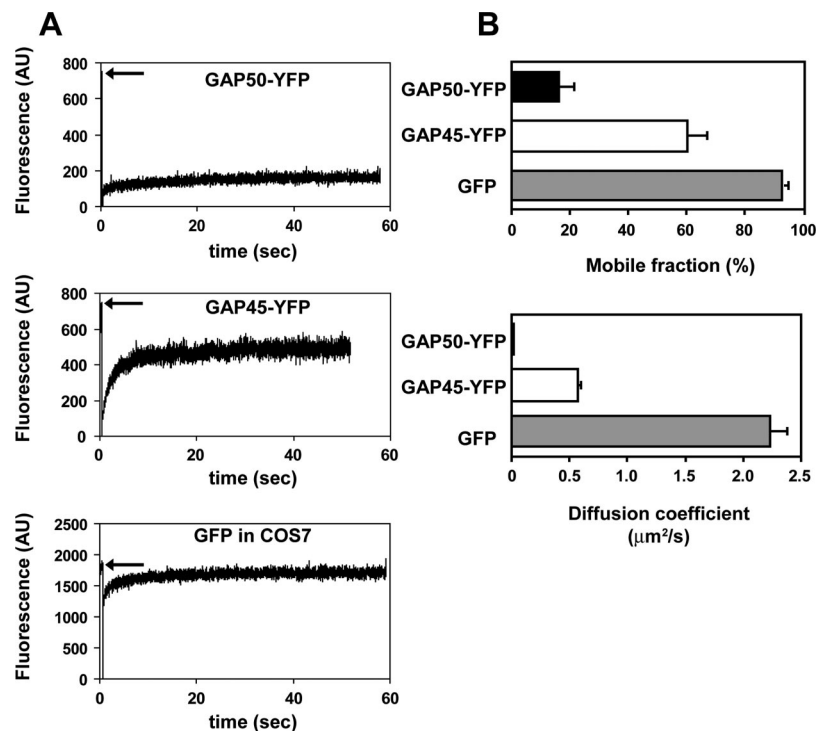

Figure 2. Quantitative analysis of GAP50-YFP mobility in the inner membrane complex. (A) Fluorescence intensity was measured as a function of time after photobleaching for GAP50-YFP and two controls: GAP45-YFP, which localizes to the IMC but does not associate with glideosome, and COS7 cells expressing GFP. Arrows indicate level of fluorescence before bleaching. (B) Mobile fractions and diffusion coefficients were averaged for all three samples confirming the slow recovery of GAP50-YFP. For GAP50-YFP, n = 9; GAP45-YFP, n = 6; and COS7 with GFP, n = 3. AU, arbitrary unit.

TgGAP45-YFP and cytosolic GFP, respectively (Figure 2B). We did not observe a complete recovery of TgGAP45–YFP, an effect that seems to be due to a substantial fraction of the total protein being bleached. From these data, we can conclude that TgGAP50, and therefore the glideosome, is immobilized within the plane of the IMC.

Glideosome Immobilization Does Not Seem to Be a Result of Protein–Protein Interactions

There are essentially two general mechanisms through which immobilization of the glideosome in the plane of the IMC membrane could be accomplished: protein–protein or protein–lipid interactions or a theoretical combination of the two. The glideosome behaves as a ~230-kDa protein complex during velocity sedimentation, and radiolabeling analysis found the four proteins in a ratio of ~1:1:1:1, indicating it is a single heterotetramer, consisting of one copy of each of the four proteins (data not shown; Gaskins *et al.*, 2004). Interaction of the four known glideosome subunits with other proteins could not be excluded, because these interactions could either be generally weak or very sensitive to the lysis and immunoprecipitation conditions used. To test this hypothesis, we subjected parasites to a number of cross-linking reagents or prepared lysates in the presence of a variety of detergents, salts, and a number of potential cofactors. None of these conditions had a reproducible effect on the number and identity of proteins in the glideosome (Supplemental Table 1), suggesting that the glideosome only consists of the four known proteins TgGAP50, TgGAP45, TgMyoA, and TgMLC1. Although the subpellicular microtubules of *Toxoplasma* are located on the opposite side of the IMC, we also tested whether they might play a role in immobilization of the glideosome. Treatment of parasites with the microtubule-disrupting drug oryzalin (Morrissette and Sibley, 2002) has no effect on anchoring of TgGAP50–YFP (data not shown). Together, these data indicate that protein–protein interactions are unlikely to play an important part in immobilization of the *Toxoplasma* glideosome in the IMC.

The Glideosome Is Found in Detergent-resistant Domains of the IMC

During our exploration of various glideosome solubilization methods, we noticed striking differences in the efficiency of glideosome extraction by different detergents. A variety of detergents, such as β-octylglucoside and CHAPS, solubilized the glideosome proteins efficiently in various buffers and at temperatures between 0 and 37°C. Triton-X100 in Tris-buffered saline (TX100/TBS) also solubilized the glideosome efficiently in the same temperature range. When parasites were subjected to extraction with 1% Triton-X100 in phosphate-buffered saline (TX100/PBS), however, we noted that glideosome proteins were solubilized efficiently at temperatures between 25 and 37°C but that they remained insoluble when the extraction was performed at 4°C (Figure 3). To determine whether this effect reflected a general property of *Toxoplasma* membranes or membrane proteins, we also tested the behavior of the plasma membrane protein SAG1, the rhoptry protein ROP2, the dense granule protein GRA3, and *Toxoplasma* BiP by using a sequential extraction process with TX100/PBS and TX100/TBS (Figure 4A). Contrary to our observations with TgGAP50, extraction of parasites with TX100/PBS at 4°C resulted in the complete solubilization of SAG1, GRA3, ROP2, and BiP (Figure 4B). The membrane skeleton protein IMC1 remained, as expected, completely insoluble under either condition (Figure 4B). These results indicate that the insolubility of TgGAP50 in
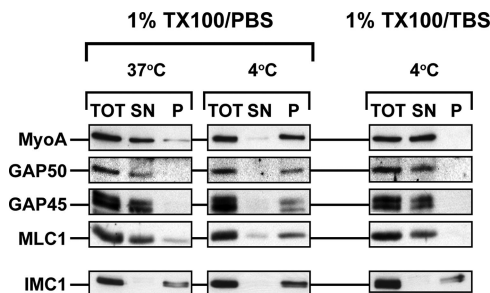

Figure 3. Glideosome solubility in Triton-X100 is temperature and buffer dependent. Parasites were harvested and subjected to detergent extraction in either 1%TX100 in PBS or 1%TX100 in TBS. Extractions were performed for 10 min at 37°C or on ice. Extracts were subjected to centrifugation for 10 min at 14,000 × *g* and 4°C. Proteins in the total lysate (TOT), supernatant (SN), and pellet (P) fractions were resolved by SDS-PAGE, transferred to nitrocellulose, and incubated with antisera to glideosome proteins and the membrane skeleton protein IMC1.

TX100/PBS on ice reflects a specific property of TgGAP50 and/or the IMC membrane it is embedded in.

To test these possibilities, we extracted parasites at 4°C in either TX100/PBS or TX100/TBS, and we examined these by light and transmission electron microscopy. As can be seen in Figure 8A, the subcellular distribution of TgGAP50–YFP is not affected in an obvious manner by extraction of parasites in TX100/PBS at 4°C, whereas it is completely lost upon extraction in TX100/TBS. Analysis by transmission electron microscopy (Figure 5) demonstrates that the plasma membrane and most organellar membranes of the parasite are solubilized efficiently in TX100/PBS. The IMC membrane, however, seems to be largely resistant to extraction by TX100/PBS and can be seen as large sheets of double membranes that are still located adjacent to the underlying cy-
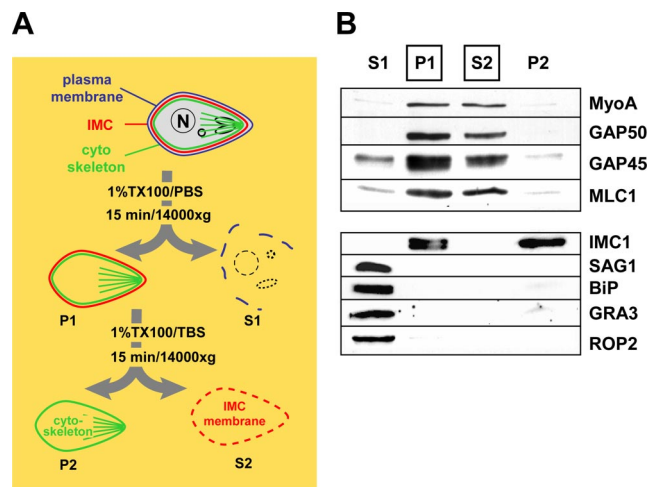

Figure 4. Sequential extraction of the glideosome from *T. gondii*. (A) Diagram of the differential solubilization of *Toxoplasma* structures during sequential extraction in 1% TX100/PBS (S1 and P1) and 1% TX100/TBS (S2 and P2). (B) Fractions obtained during these extractions were analyzed by immunoblots for the presence of the glideosome subunits (TgMyoA, TgGAP50, TgGAP45, and TgMLC1) and marker proteins for the membrane skeleton (IMC1), plasma membrane (SAG1), endoplasmic reticulum (BiP), dense granules (GRA3), and rhoptries (ROP2). The fractions containing glideosome proteins (P1 and S2) are boxed.
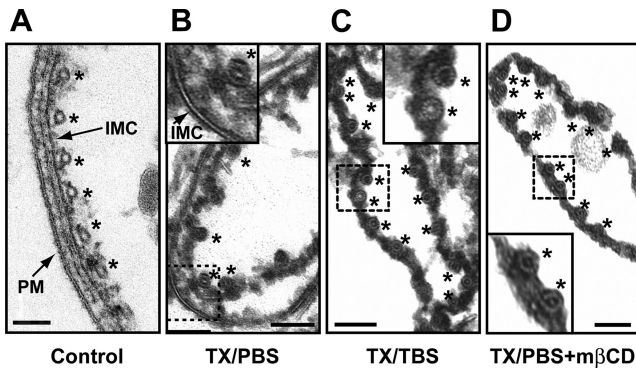
Figure 5. The IMC membrane is largely resistant to extraction by TX100/PBS. (A) Isolated pellicles of nonextracted parasites possess an intact plasma membrane, IMC membrane, and the associated cytoskeleton. (B) Extraction in TX100/PBS removes the plasma membrane but does not affect the appearance of the IMC membrane. (C) The IMC membrane is solubilized efficiently by extraction in TX100/TBS as well as by treatment with mβCD (D). Subpellicular microtubules are indicated by asterisks. Bar, 100 nm.

toskeleton. Extraction of parasites with TX100/TBS, in contrast, resulted in the complete solubilization of *Toxoplasma* membranes, including the IMC membrane (Figure 5C).

To provide further proof that the detergent-resistant fraction of TgGAP50-YFP is indeed membrane associated, we subjected this material to isopycnic centrifugation. The TX100/PBS-resistant material was adjusted to 1.6 M sucrose, placed underneath a 0.25–1.4 M sucrose gradient, and it was subjected to equilibrium density gradient centrifugation. Whereas the cytoskeletal protein IMC1 and α-tubulin remained at the bottom of the gradient, TgGAP50 was found exclusively at lower density fractions (density ~1.1 M sucrose), indicating that it is present in membranes or lipid-rich structures (Figure 6). TgMyoA, TgGAP45, and TgMLC1 were also found in this fraction, indicating all proteins of the glideosome are similarly immobilized with TgGAP50. When the TX100/PBS-resistant material was incubated in TX100/TBS before centrifugation, TgGAP50 and glideosome proteins remained at the bottom of the gradient (data not shown). Together with our previous observations, these data support a model in which the *Toxoplasma* glideosome is immobilized in detergent-resistant domains in the parasites' IMC membranes.
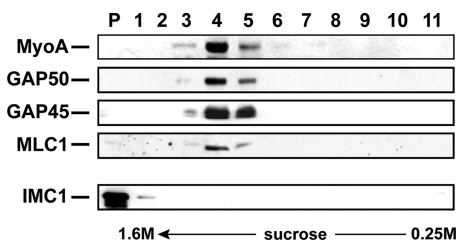

Figure 6. Sucrose density gradient centrifugation analysis of the TX100/PBS-resistant IMC fraction. Parasites were lysed in 1% TX100 in PBS on ice and the TX100-soluble and -insoluble material was separated by differential centrifugation. The pellet fraction was resuspended, adjusted to 1.6 M sucrose, overlaid with a gradient of 1.4, 1.2, 1.1, 1.0, 0.9, 0.8, 0.7, 0.6, and 0.25 M sucrose and subjected to centrifugation for 2 h at 120,000 × *g*. Fractions were collected from the bottom of the gradient and analyzed by SDS-PAGE and immunoblotting for IMC1 and TgGAP50.
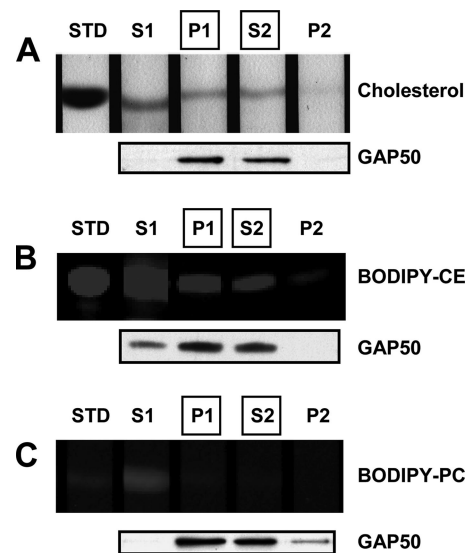
Figure 7. Cholesterol is selectively enriched in the *Toxoplasma* IMC. Parasites were harvested and incubated with no dye (A), BODIPY-CE (B), or BODIPY-PC (C) for 3 h at 37°C. Sequential detergent extractions were performed as described for Figure 4 by using 1% TX100 in PBS (S1 and P1) followed by 1% TX100 in TBS (S2 and P2), both on ice. Lipids were extracted from all fractions and analyzed by TLC. The extraction efficiency of TgGAP50 in these buffers was confirmed by immunoblot analysis. STD, lipid standard.

The Presence of Cholesterol Correlates with the Immobilization of Glideosome in the IMC Membrane

Detergent-resistant membrane (DRM) domains in other eukaryotes are thought to be formed by the tight packing of cholesterol and the long and highly saturated fatty acids of sphingolipids, and they contain a variety of proteins, including GPI-anchored, acylated, and integral membrane proteins (for review, see Pike, 2004). To determine whether the TX100/PBS-resistant IMC membranes of *Toxoplasma* also contained high concentrations of cholesterol, we compared the lipid composition of total parasite membranes and the TX100/PBS-soluble and insoluble fractions by TLC. The extraction efficiency of TgGAP50 was monitored in parallel by immunoblot analysis. As can be seen in Figure 7A, a substantial fraction of the total parasite-associated cholesterol is resistant to extraction in TX100/PBS, but it is solubilized completely by a subsequent extraction in TX100/TBS. To determine whether the TX100/PBS-resistant fraction of cholesterol was indeed associated with the *Toxoplasma* IMC, we labeled parasites before extraction with BODIPY-CE, a fluorescent cholesterol derivative that is commonly used as a qualitative tool to describe the subcellular distribution of cholesterol. As a control, parasites were also labeled with BODIPY-PC to provide a marker for other parasite membranes.

As has been described previously (Coppens and Joiner, 2003), BODIPY-CE seems to accumulate in the *Toxoplasma* pellicle and in internal organelles that are consistent with the parasite rhoptries (Figure 8A). BODIPY-PC, in contrast, was found in membranes throughout the parasite (Figure 8B). Treatment of parasites with TX100/PBS resulted in a complete removal of parasite-associated BODIPY-PC as judged by both TLC analysis (Figure 7C) and fluorescence microscopy (Figure 8B). As we had already described for endogenous cholesterol, TLC analysis revealed that a substantial fraction of parasite-associated BODIPY-CE was retained af-
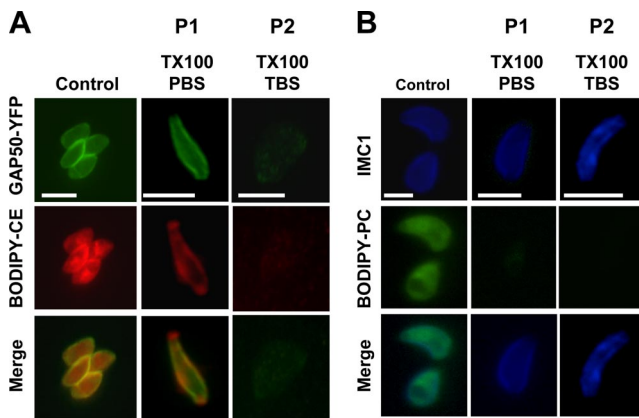
Figure 8. The TX100/PBS-resistant cholesterol and TgGAP50 in the IMC are efficiently extracted with TX100 in TBS. (A) BODIPY-cholesteryl ester accumulates in the *Toxoplasma* IMC, as judged by the overlap with GAP50. IMC-associated BODIPY-CE is resistant to extraction by TX100/PBS but is solubilized by TX100/TBS. (B) BODIPY-PC is found throughout the parasite and is completely extracted in TX100/PBS. P1 and P2 refer to extraction performed as in Figure 4. Bar, 5 μm.

ter extraction in TX100/PBS (Figure 7B). Fluorescence microscopy revealed that this pool of BODIPY-CE was associated primarily with the parasite IMC as judged by the extensive overlap in distribution with TgGAP50-YFP (Figure 8A). A fraction of the fluorescent lipid also seemed to be associated with the extreme apical region of the parasite where TgGAP50-YFP was absent, suggesting this may represent a unique domain of the IMC membrane. When the TX100/PBS extraction was followed by extraction in TX100/TBS both BODIPY-CE and TgGAP50 were completely extracted, confirming that both are indeed associated with membranes (Figure 8A).
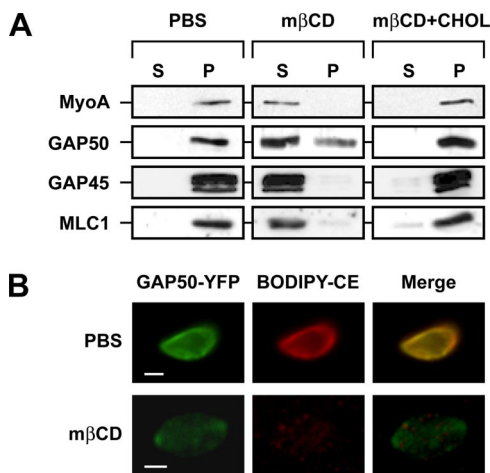

Figure 9. TX100/PBS-resistant cholesterol and TgGAP50 are completely extracted by mβCD. (A) The TX100/PBS-resistant fraction was incubated in PBS or in PBS containing 30 mM mβCD or 30 mM mβCD and 5 μg of cholesterol (CHOL) for 30 min at 37°C. TritonX-100 was added to 1%, and parasites were incubated on ice for 10 min. Soluble and insoluble fractions were separated by centrifugation at 14,000 × g for 10 min at 4°C and analyzed for the presence of TgGAP50 by SDS-PAGE and immunoblot analysis. (B) The TX100/PBS-resistant fraction of parasites prelabeled with BODIPY-CE was incubated in the presence or absence of 30 mM mβCD for 45 min at 37°C and analyzed by fluorescence microscopy. Bar, 2 μm.

It is clear from the aforementioned findings that both cholesterol and the glideosome resist extraction by TX100/PBS and that they are solubilized efficiently by TX100/TBS. Several explanations can be offered for these observations. First, the selective retention of both components in the IMC during the initial detergent extraction step could be caused by them being embedded independently in the IMC membrane. An alternative explanation is that both components closely interact with each other and that the presence of cholesterol is critical for glideosome retention. To determine whether the presence of cholesterol indeed contributes to the retention of TgGAP50, we analyzed whether the latter was sensitive to the cholesterol-sequestering agent mβCD. Short-term incubation of intact parasites with mβCD did not affect TgGAP50, presumably because the IMC membranes are shielded by the parasite plasma membrane. Incubation of TX100/PBS-extracted parasites with mβCD, in contrast, resulted in the solubilization of TgGAP50 as judged by immunoblotting and fluorescence microscopy (Figure 9). All other members of the glideosome (TgMyoA, TgGAP45, and TgMLC1) were also solubilized in a similar manner as Tg-GAP50, indicating that the motor itself remains tightly associated to TgGAP50 in the IMC. Examination of the mβCD-treated parasites by electron microscopy revealed that cholesterol depletion actually results in the complete removal of the TX100/PBS-resistant IMC membranes (Figure 5). The effect of mβCD on TgGAP50 solubilization was due to its ability to sequester cholesterol, because it was prevented by the addition of free cholesterol (Figure 9A). These observations indicate that cholesterol is clearly a very important structural element of the IMC membrane and that it is critical for the retention of the glideosome in that membrane.

DISCUSSION

Motility of *Toxoplasma* and other apicomplexan parasites depends on the activity of the MyoA myosin heavy chain and the associated myosin light chain-like protein MLC1, both of which are found in a complex with GAP45 and GAP50 (Gaskins *et al.*, 2004). A general conservation of the glideosome components has been demonstrated between at least six apicomplexan genera, indicating that this complex plays an essential role in the invasion and motility of these protozoan parasites (Bergman *et al.*, 2003; Gaskins *et al.*, 2004). This notion is supported by the observation that *Toxoplasma* is not viable after the individual disruption of three glideosome subunits: TgMyoA, TgGAP45, and TgGAP50 (Meissner *et al.*, 2002; Gaskins *et al.*, 2004).

We have demonstrated previously that the integral membrane protein TgGAP50 anchors the glideosome complex in the *Toxoplasma* IMC, which consists of large flattened cisternae that underlie the parasite plasma membrane (Gaskins *et al.*, 2004). It was not clear, however, whether and how Tg-GAP50 and therefore the entire glideosome was immobilized in the plane of the IMC membrane, a prerequisite for net movement of the parasite with respect to its substrate. We have demonstrated here that TgGAP50 is indeed immobilized within the plane of the IMC and that the presence of cholesterol in the IMC membrane seems to play a role in this process.

We determined the extent of TgGAP50 immobilization in the plane of the IMC membranes by FRAP analysis of the fusion protein TgGAP50-YFP, in which YFP is attached to the short C-terminal cytoplasmic tail of TgGAP50. This fusion protein seems to be fully functional in that it is indistinguishable from TgGAP50 in its targeting to the IMC and

its association with TgMyoA, TgMLC1, and TgGAP45 (Gaskins *et al.*, 2004). Judged by our FRAP analysis, Tg-GAP50 does not diffuse freely within the plane of the IMC membranes. This is not the result of general diffusion barriers within the parasite or the IMC membrane, as proteins associated with the IMC membrane through acylation (Tg-GAP45-YFP) are able to recover within seconds. This observation proves that TgGAP50 is effectively immobilized in the IMC membrane. We considered several explanations for this observation. Stable cytoskeletal structures have not been described on the side of the IMC where the glideosome is located, the side facing the parasite plasma membrane or in the IMC lumen, where the bulk of TgGAP50 resides. The side of the IMC facing the cytoplasm of the parasite, in contrast, is associated with a filamentous membrane skeleton and 23 subpellicular microtubules (Mann *et al.*, 2001). We tested whether the immobility of TgGAP50 was due to its interaction, or that of another glideosome subunit, with other proteins in the IMC or the associated membrane skeleton or microtubules. The use of several membrane-permeable and membrane-impermeable chemical cross-linkers in various buffer conditions and the inclusion of a variety of potential cofactors, such as ATP, GTP, calcium, and magnesium, did not alter the protein composition of the immuno-precipitated glideosome. Additionally, treatment of parasites with oryzalin, a microtubule-destabilizing drug, does not alter the extraction properties of the glideosome, indicating a tight association with the IMC despite the lack of microtubule presence. These findings suggest that glideosome immobilization is not likely to be caused by its direct interaction with other proteins in the *Toxoplasma* IMC or cytoskeleton. If an additional protein is involved, these interactions may be very weak or transient and therefore they are unlikely to be strong enough to confer anchoring within a membrane. Alternatively, an interacting protein may be large or insoluble, thereby preventing the effective cross-linking and immunoprecipitation with TgGAP50.

In doing these various experiments, we noted that solubilization of the glideosome from the IMC by the detergent Triton-X100 is temperature and buffer dependent. The glideosome was efficiently extracted from the IMC membrane using TX100 in PBS at room temperature but not on ice. This property was reminiscent of the detergent-insoluble domains or rafts described in other eukaryotes (Brown and Rose, 1992). Like the detergent-resistant structures observed in other studies, the detergent-resistant IMC fraction of *Toxoplasma* also consists of membrane-like structures. These differ from detergent-insoluble membranes in other systems, however, in that their density is substantially higher (Figure 6). We have found that this is not due to associated cytoskeletal proteins and is therefore probably a result of a higher protein/lipid ratio in the IMC membranes proper compared with DRMs in other eukaryotes. Interestingly, the temperature-dependent solubilization of the glideosome observed in TX100 in phosphate-buffered saline is not observed using TX100 in Tris-buffered saline. In this regard, the IMC membrane seems to be similar to membrane domains found in myelin. These domains were also found to be insoluble in TX100 in phosphate buffer, but they were solubilized efficiently by TX100 in a Tris-based buffer (Arvanitis *et al.*, 2005), and, like we observed for the IMC membrane, the TX100/phosphate-resistant myelin fraction was found to have a higher density than typical DRMs. It is interesting to note in this context that both the *Toxoplasma* IMC and myelin are composed of closely apposed membranes, suggesting that phosphate may play a role in their association.

Detergent-insoluble domains in other eukaryotes are characterized by a relative enrichment of cholesterol and sphingolipids (Simons and Ikonen, 1997). Analysis of the lipid composition of the TX100-resistant IMC membrane reveals that it too is enriched in cholesterol. The importance of cholesterol in the integrity of the IMC membrane and immobilization of the glideosome is illustrated by two observations. Treatment of the IMC with mβCD results in nearly complete disruption of the IMC membrane and the complete solubilization of the glideosome, without affecting the IMC-associated cytoskeleton. Sphingolipids, in contrast, do not seem to be important for glideosome immobilization in the IMC membrane, because this is not affected by sphingomyelinase treatment (data not shown). We have found that glideosome is enriched in these DRMs in the IMC, but we cannot conclude that this mechanism is fully responsible for anchoring TgGAP50.

Although other factors are likely to contribute to the immobilization of the glideosome in the IMC membrane of *Toxoplasma*, it is clear from our data that the presence of cholesterol plays a supporting role. *Toxoplasma* is a cholesterol auxotroph (Coppens *et al.*, 2000) and that it seems to acquire this lipid from its host cell through the hijacking of endocytic host cell organelles carrying low-density lipoprotein particles. These are delivered to the parasitophorous vacuole surrounding the intracellular parasites from which they are taken up by the parasite. Once inside the parasite, cholesterol has many functions. It is found in lipid bodies (Murphy, 2001), rhoptries (Foussard *et al.*, 1991; Vial *et al.*, 2003), and the IMC (Coppens and Joiner, 2003). Treatment of parasite with progesterone resulted in the depletion of cholesterol from the rhoptries and lipid bodies. These parasites still exhibited IMC labeling with filipin, a cholesterol binding agent, indicating cholesterol is not depleted from this structure by progesterone treatment (Coppens and Joiner, 2003). When we attempted to extract cholesterol from intact parasites with mβCD, we also found that it was impossible to remove this lipid from the IMC. This particular observation is most likely due to the failure of mβCD to gain access to the IMC membrane in intact parasites. Both observations made it impossible for us to assess the effect of cholesterol depletion on motility of the intact parasite. When we first removed the parasite plasma membrane with TX100/PBS, however, mβCD extracted cholesterol efficiently from the TX100/PBS-resistant IMC membranes and resulted in a complete solubilization of the glideosome.

It is clear from these observations that cholesterol is involved in immobilization of the *Toxoplasma* glideosome in the IMC membrane. It is equally clear, however, that this raises many new questions. Chief among these questions is whether glideosome immobilization involves a direct interaction of cholesterol and TgGAP50, or whether it is due to the effect of cholesterol on the IMC membrane per se. Because TgGAP50 is an abundant protein in the IMC membrane, it is possible that the monomers are packed so closely together that a lattice of TgGAP50 molecules is created and stabilized by cholesterol. Removal of the cholesterol would then render the lattice unstable and prone to disruption by detergents. The possibility that the actual lipid composition, and specifically the presence of cholesterol, turns the IMC membrane into an unusually rigid structure that immobilizes TgGAP50 cannot be excluded at this point either, although it is unlikely that this is the only factor involved.

A second issue that needs addressing in this context is the organization of the detergent-resistant fraction of the IMC membrane. In other experimental models, these domains have been estimated to range in size from 40 to >500 nm

(Brown and Lyles, 2003; Gupta and DeFranco, 2003; Prior *et al.*, 2003) and to constitute up to 35% of a plasma membrane (Prior *et al.*, 2003), depending on the cell type and isolation method used (Lucero and Robbins, 2004). Fluorescence and electron microscopy indicate that the overall appearance of the IMC membrane is not grossly affected by extraction in TX/PBS (Figures 5 and 8). It is therefore possible that this membrane is detergent-resistant in its entirety. It can also be, however, that the IMC membrane resembles packed ice in that it consists of numerous smaller detergent-resistant domains that float as a closely packed aggregate in an otherwise detergent-sensitive membrane.

Finally, the overall composition of the detergent-resistant domains also remains to be determined. Although cholesterol is clearly an important constituent, other lipids or proteins may play equally important roles in the formation and maintenance of this structure. It is also likely that, apart from immobilizing the glideosome, the unusual IMC membrane domains we described here may play equally important roles in the localization and function of other factors required for parasite survival and its ability to cause disease.

ACKNOWLEDGMENTS

REFERENCES

Arvanitis, D. N., Min, W., Gong, Y., Heng, Y. M., and Boggs, J. M. (2005). Two types of detergent-insoluble, glycosphingolipid/cholesterol-rich membrane domains from isolated myelin. J. Neurochem. *94*, 1696–1710.

Baum, J., Richard, D., Healer, J., Rug, M., Krnajski, Z., Gilberger, T. W., Green, J. L., Holder, A. A., and Cowman, A. F. (2006). A conserved molecular motor drives cell invasion and gliding motility across malaria life cycle stages and other apicomplexan parasites. J. Biol. Chem. *281*, 5197–5208.

Bergman, L. W., Kaiser, K., Fujioka, H., Coppens, I., Daly, T. M., Fox, S., Matuschewski, K., Nussenzweig, V., and Kappe, S. H. (2003). Myosin A tail domain interacting protein (MTIP) localizes to the inner membrane complex of *Plasmodium* sporozoites. J. Cell Sci. *116*, 39–49.

Bligh, E. G., and Dyer, W. J. (1959). A rapid method of total lipid extraction and purification. Can J. Biochem. Physiol. *37*, 911–917.

Bosch, J., *et al.* (2006). Structure of the MTIP-MyoA complex, a key component of the malaria parasite invasion motor. Proc. Natl. Acad. Sci. USA *103*, 4852–4857.

Brown, D. A., and Rose, J. K. (1992). Sorting of GPI-anchored proteins to glycolipid-enriched membrane subdomains during transport to the apical cell surface. Cell *68*, 533–544.

Brown, E. L., and Lyles, D. S. (2003). A novel method for analysis of membrane microdomains: vesicular stomatitis virus glycoprotein microdomains change in size during infection, and those outside of budding sites resemble sites of virus budding. Virology *310*, 343–358.

Coppens, I., and Joiner, K. A. (2003). Host but not parasite cholesterol controls Toxoplasma cell entry by modulating organelle discharge. Mol. Biol. Cell *14*, 3804–3820.

Coppens, I., Sinai, A. P., and Joiner, K. A. (2000). *Toxoplasma gondii* exploits host low-density lipoprotein receptor-mediated endocytosis for cholesterol acquisition. J. Cell Biol. *149*, 167–180.

Dobrowolski, J. M., and Sibley, L. D. (1996). *Toxoplasma* invasion of mammalian cells is powered by the actin cytoskeleton of the parasite. Cell *84*, 933–939.

Dubey, J. P. (1994). Toxoplasmosis. J. Am. Vet. Med. Assoc. *205*, 1593–1598.

Foussard, F., Leriche, M. A., and Dubremetz, J. F. (1991). Characterization of the lipid content of *Toxoplasma gondii* rhoptries. Parasitology *102*, 367–370.

Gaskins, E., Gilk, S., DeVore, N., Mann, T., Ward, G., and Beckers, C. (2004). Identification of the membrane receptor of a class XIV myosin in *Toxoplasma gondii*. J. Cell Biol. *165*, 383–393.

Gordon, G. W., Berry, G., Liang, X. H., Levine, B., and Herman, B. (1998). Quantitative fluorescence resonance energy transfer measurements using fluorescence microscopy. Biophys. J. *74*, 2702–2713.

Gupta, N., and DeFranco, A. L. (2003). Visualizing lipid raft dynamics and early signaling events during antigen receptor-mediated B-lymphocyte activation. Mol. Biol. Cell *14*, 432–444.

Heintzelman, M. B., and Schwartzman, J. D. (1999). Characterization of myosin-A and myosin-C: two class XIV unconventional myosins from *Toxoplasma gondii*. Cell Motil. Cytoskeleton *44*, 58–67.

Herm-Gotz, A., Weiss, S., Stratmann, R., Fujita-Becker, S., Ruff, C., Meyhofer, E., Soldati, T., Manstein, D. J., Geeves, M. A., and Soldati, D. (2002). Toxoplasma gondii myosin A and its light chain: a fast, single-headed, plus-end-directed motor. EMBO J. *21*, 2149–2158.

Jewett, T. J., and Sibley, L. D. (2003). Aldolase forms a bridge between cell surface adhesins and the actin cytoskeleton in apicomplexan parasites. Mol. Cell *11*, 885–894.

Kappe, S., Bruderer, T., Gantt, S., Fujioka, H., Nussenzweig, V., and Menard, R. (1999). Conservation of a gliding motility and cell invasion machinery in apicomplexan parasites. J. Cell Biol. *147*, 937–944.

Lucero, H. A., and Robbins, P. W. (2004). Lipid rafts-protein association and the regulation of protein activity. Arch. Biochem. Biophys. *426*, 208–224.

Mann, T., and Beckers, C. (2001). Characterization of the subpellicular network, a filamentous membrane skeletal component in the parasite *Toxoplasma gondii*. Mol. Biochem. Parasitol. *115*, 257–268.

Mann, T., Gaskins, E., and Beckers, C. (2002). Proteolytic processing of TgIMC1 during maturation of the membrane skeleton of *Toxoplasma gondii*. J. Biol. Chem. *277*, 41240–41246.

Meissner, M., Schluter, D., and Soldati, D. (2002). Role of *Toxoplasma gondii* myosin A in powering parasite gliding and host cell invasion. Science *298*, 837–840.

Morrissette, N. S., and Sibley, L. D. (2002). Disruption of microtubules uncouples budding and nuclear division in *Toxoplasma gondii*. J. Cell Sci. *115*, 1017–1025.

Moudy, R., Manning, T. J., and Beckers, C. J. (2001). The loss of cytoplasmic potassium upon host cell breakdown triggers egress of *Toxoplasma gondii*. J. Biol. Chem. *276*, 41492–41501.

Murphy, D. J. (2001). The biogenesis and functions of lipid bodies in animals, plants and microorganisms. Prog. Lipid Res. *40*, 325–438.

Pike, L. J. (2004). Lipid rafts: heterogeneity on the high seas. Biochem. J. *378*, 281–292.

Prior, I. A., Muncke, C., Parton, R. G., and Hancock, J. F. (2003). Direct visualization of Ras proteins in spatially distinct cell surface microdomains. J. Cell Biol. *160*, 165–170.

Rees-Channer, R. R., Martin, S. R., Green, J. L., Bowyer, P. W., Grainger, M., Molloy, J. E., and Holder, A. A. (2006). Dual acylation of the 45 kDa gliding-associated protein (GAP45) in *Plasmodium falciparum* merozoites. Mol. Biochem. Parasitol. *149*, 113–116.

Simons, K., and Ikonen, E. (1997). Functional rafts in cell membranes. Nature *387*, 569–572.

Soldati, D., and Meissner, M. (2004). *Toxoplasma* as a novel system for motility. Curr. Opin. Cell Biol. *16*, 32–40.

Vial, H. J., Eldin, P., Tielens, A. G., and van Hellemond, J. J. (2003). Phospholipids in parasitic protozoa. Mol. Biochem. Parasitol. *126*, 143–154.